IEEE Photonics Journal
An IEEE Photonics Society Publication

Open Access

Simultaneous Measurement of Axial Strain and Temperature Based on a Z-Shape Fiber Structure

Volume 9, Number 4, August 2017

Chi Zhang
Ping Lu
Hao Liao
Wenjun Ni
Xin Fu
Xinyue Jiang
Deming Liu
Jiangshan Zhang

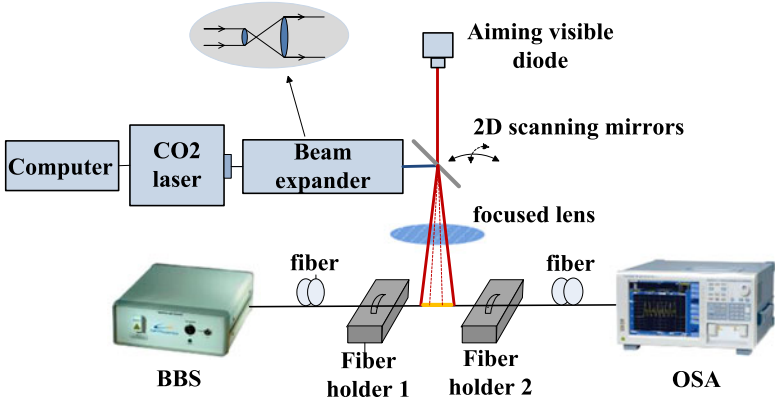

DOI: 10.1109/JPHOT.2017.2727540
1943-0655 © 2017 IEEE

Simultaneous Measurement of Axial Strain and Temperature Based on a Z-Shape Fiber Structure

Chi Zhang,[1,2] Ping Lu,[1,2] Hao Liao,[1,2] Wenjun Ni,[1,2] Xin Fu,[1,2] Xinyue Jiang,[1,2] Deming Liu,[1,2] and Jiangshan Zhang[3]

[1]Wuhan National Laboratory for Optoelectronics, Huazhong University of Science and Technology, Wuhan 430074, China
[2]School of Optical and Electronic Information, National Engineering Laboratory for Next Generation Internet Access System, Huazhong University of Science and Technology, Wuhan 430074, China
[3]Department of Electronics and Information Engineering, Huazhong University of Science and Technology, Wuhan 430074, China

DOI:10.1109/JPHOT.2017.2727540

Manuscript received February 13, 2017; revised June 15, 2017; accepted July 12, 2017. Date of publication July 17, 2017; date of current version July 25, 2017. This work was supported in part by the National Natural Science Foundation of China under Grants 61275083, 61290315, and 61290311, and in part by the Fundamental Research Funds for the Central Universities under Grant 2017KFYXJJ032.
Corresponding author: P. Lu (e-mail: pluriver@mail.hust.edu.cn).

Abstract: A Z-shape fiber structure fabricated by CO_2 laser is proposed here for the simultaneous measurement of axial strain and temperature. The Z-shape structure is fabricated by simply exposing a single mode fiber (SMF) to the focused CO_2 laser that causes the unbalanced residual stress relaxation between the upper surface and lower surface of the fiber. The laser irradiation also gives rise to efficient coupling between the core mode and cladding modes. Then, a Mach–Zehnder interferometer is prepared. Experiments and theoretical analyses have been carried out to verify the feasibility of applying the proposed structure to simultaneous strain and temperature measurement. Experimental results indicate that the sensitivities of strain and temperature obtained by the two resonant dips are 129.78 pm/$\mu\epsilon$, 43.57 pm/°C, and 51.05 pm/$\mu\epsilon$, 62.1 pm/°C, respectively. Thanks to its highly sensitive spectral response, the proposed sensor will have attractive potential applications in dual parameter fiber sensing.

Index Terms: CO_2 laser, strain, temperature, Z-shape structure.

1. Introduction

In-line optical fiber sensors have been extensively investigated in the last decades. Numerous types of in-line optical fiber sensors have emerged and been employed in various sensing applications, such as refractive index [1], temperature [2], strain [3], humidity [4], curvature [5] and so on. They are low-cost, highly sensitive, stable, and immune to electromagnetic interference, making them formidable competitors to conventional electronic sensors. Among these, in-line Mach-Zehnder interferometer (MZI) stands out due to its compact size, flexible design and low cost. It contains two coupling components which act as the beam splitter and combiner to form interference pattern. In the past decades, MZIs are widely used for simultaneous measurement of strain and temperature which is of great importance for many fields, such as environmental monitoring, structure inspection, road

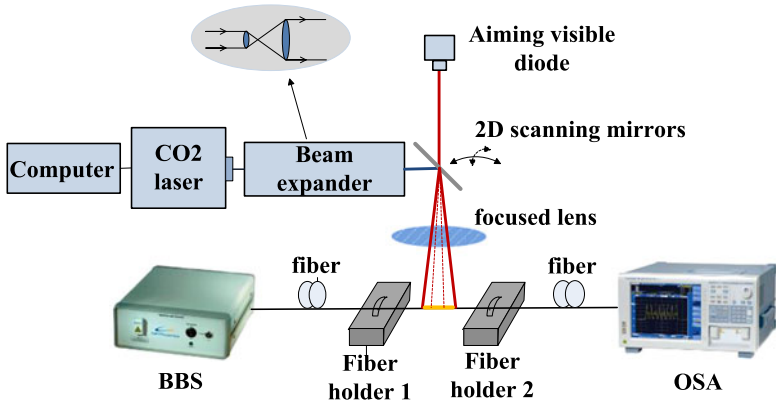

Fig. 1. The schematic diagram of CO_2 laser platform.

construction and so on. Different coupling elements of MZIs are designed to realize dual parameter measurement. Ping Lu [6] proposed a kind of MZI consisting of a fiber taper and a lateral-shift junction that achieved the simultaneous measurement of strain and temperature. Di Wu [7] presented a scheme based on cascaded peanut-shape structure and a relative high sensitivity was obtained. And there are many other structures such as special fiber [8], fiber Bragg grating [9], long period fiber grating [10] etc. However, the in-line MZIs mentioned above need high-cost special fibers, use fragile structures like abrupt tapers and microfibers, or have critical requirements on devices. Moreover, the measured strain sensitivity typically is less than 10 pm/$\mu\varepsilon$. How to design a sensitive and stable fiber structure is an important issue that should be solved urgently in the practical application.In this paper, we demonstrate a Z-shape fiber structure fabricated by CO_2 laser for simultaneous measurement of strain and temperature. CO_2 laser processing method is particularly flexible, as it is applicable to different types of fibers and can be controlled easily to produce various structures. The laser irradiation causes light coupling from the core mode to cladding modes and vise versa. The sensor proposed just consists of a segment of normal single mode fiber (SMF) which is inexpensive and easy to fabricate. The highly sensitive spectral response makes it possible to realize the precise dual parameter measurement in small variation range. As the structure is fabricated without splicing or tapering, it is firmer compared to many other sensors and applicable in high strength sensing circumstances. Owing to its compact size, high sensitivity and robustness, it will have attractive potential applications in the fields of structural deformation and mechanical engineering.

2. Fabrication and Simulation

Schematic diagram of the experimental setup is shown in Fig. 1. To fabricate the Z-shape structure, a platform based on CO_2 laser is built. The CO_2 laser (Synrad 48-2) is controlled by self-developed program so that accurate adjustment of exposure time and output power can be achieved. Then CO_2 laser beam diameter is expanded three times from 3.5 mm to 10.5 mm by the lens assembly. An aiming visible laser diode is adopted in the system to indicate the invisible CO_2 laser. The heating source applied on the single SMF is a strip laser focused and swept by F-theta focused lens and 2-dimentional scanning mirrors, respectively. The expanding and focusing process towards laser beam is adopted to reduce beam divergence and improve beam quality. It should be pointed out that the 2-dimentional scanning mirrors are used to adjust the laser spot location and realize high speed scanning of laser. In addition, the strip laser must be adjusted to be parallel to the single SMF. When the strip light focuses onto the single SMF, it brings about relaxation of residual stress which already exists in the fiber after drawing [11]. Owing to the one-sided laser exposure, it is out of balance of residual stress relaxation between the fiber upper surface and lower surface. Finally Z-shape fiber structure is prepared.

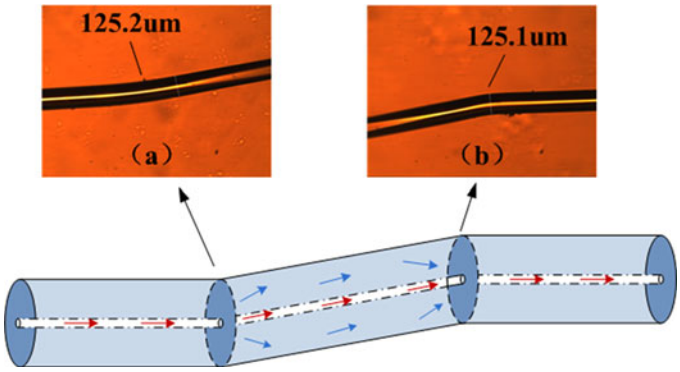

Fig. 2. Z-shape structure (a) the left part (b) the right part.

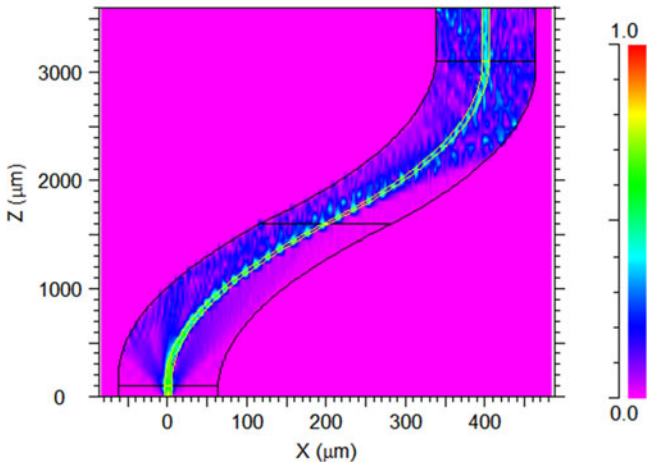

Fig. 3. Simulated light energy distribution in the Z-shape structure

Several Z-shape structures with different laser parameters are fabricated and experimentally tested. We choose the sample with the highest sensitivity to get the optimal laser parameters.

At last the output power, exposure time and laser beam size are set as 9 W, 1 s and 500 μm $*$ 3.5 mm, respectively. Fig. 2(a) and (b) exhibits the microscope image of the left and right part of the Z-shape structure. Owing to the relative long length about 3.5 mm, the full image can't be displayed by the microscope. The diameter along the whole structure is found almost unchanged to be about 125 μm after laser irradiation. Only tiny diameter change happens in the two bending points. It should be mentioned that the Z-shape structure is similar to S-taper [12]. There exist some differences. The first one is the fabrication method and forming mechanism. S-taper structure is fabricated by fusion splicer by introducing axial offset, splicing and tapering. Z-shape structure is made by CO_2 laser. Its unique structure is formed by the unbalanced residual stress relaxation between the fiber upper surface and lower surface owing to one-sided laser exposure of CO_2 laser. The second one is the essential structure difference. The waist of S-taper is about tens of microns and there exists a splicing joint in the middle of S-taper. But the diameter of Z-shape is almost unchanged of about 125 μm. It should be firmer than many taper-based sensors because no tapers or splicing joints exist along the fiber. It will have potential applications in harsh environments.

Fig. 3 shows the simulated light energy distribution in the Z-shape structure using finite element beam propagation method. The parameters of Z-shape are obtained from Fig. 2. The total length, offset and diameter are set to be 3.5 mm, 400 μm and 125 μm, respectively. According to the

simulation, we can clearly see that a fraction of light energy is coupled from the fiber core to fiber cladding in the first bending region, then part of light is coupled back from the fiber cladding to fiber core in the second bending region. The bending regions act as the beam splitter and combiner. Due to the effective refractive index difference between core mode and cladding modes, a typical in-line MZI is formed.

Providing that several cladding modes take part in the interference, the light intensity can be expressed as:

$$I = I_{co} + \sum_j I^j_{clad} + 2\sum_j \sqrt{I_{co} I^j_{clad}} \cos(\Delta\varphi_j) \tag{1}$$

where I_{co}, I_{clad} are the light intensity of core mode and *j*-th cladding mode, $\Delta\varphi_j$ is the phase difference between core mode and *j*-th cladding mode.

$$\Delta\varphi_j = \frac{2\pi}{\lambda} \Delta n^j_{eff} L_{eff} \tag{2}$$

where λ is the wavelength of incident light, Δn_{eff} is the effective refractive index difference between core mode and *j*-th cladding mode, L_{eff} is the effective interferometer length. The attenuation peak wavelength can be calculated when $\Delta\varphi_j$ becomes $(2m + 1)\pi$. It can be expressed as follows:

$$\lambda_m = \frac{2\Delta n^j_{eff} L_{eff}}{2m + 1} \tag{3}$$

where *m* is a positive integer.

Free Spectral Range (*FSR*) can be figured out as:

$$FSR = \frac{\lambda^2}{\Delta n^j_{eff} L_{eff}} \tag{4}$$

According to above-mentioned equations, we can analyze the interference process further. When a strain is applied to the fiber sensor or ambient temperature changes, the fiber length and mode indices will change accordingly. By conducting differential operation to (3), we have

$$\frac{\Delta\lambda_m}{\lambda_m} = \left[\frac{1}{\Delta n_{eff}} \frac{\partial(\Delta n_{eff})}{\partial T} + \frac{1}{L}\frac{\partial L}{\partial T}\right] \Delta T + \left[1 + \frac{1}{\Delta n_{eff}} \frac{\partial(\Delta n_{eff})}{\partial \varepsilon}\right] \Delta\varepsilon \tag{5}$$

where ϵ indicates the applied strain and T indicates the ambient temperature. The resonant wavelengths will shift as we can tell in (5). And the shifts of resonant wavelengths can be expressed as

$$\begin{pmatrix} \Delta\lambda_1 \\ \Delta\lambda_2 \end{pmatrix} = \begin{pmatrix} K_{1\varepsilon} & K_{1T} \\ K_{2\varepsilon} & K_{2T} \end{pmatrix} \begin{pmatrix} \Delta\varepsilon \\ \Delta T \end{pmatrix} = M \begin{pmatrix} \Delta\varepsilon \\ \Delta T \end{pmatrix} \tag{6}$$

where $\Delta\lambda_1$, $\Delta\lambda_2$ are the wavelength shifts, $K_{1\epsilon}$, $K_{2\epsilon}$ are the strain coefficients, K_{1T}, K_{2T} are the thermal coefficients of different resonant dips and *M* is the coefficient matrix. The parameters mentioned can be obtained by experiments. Then the applied strain and temperature change can be simultaneously calculated from (6):

$$\begin{pmatrix} \Delta\varepsilon \\ \Delta T \end{pmatrix} = M^{-1} \begin{pmatrix} \Delta\lambda_1 \\ \Delta\lambda_2 \end{pmatrix} \tag{7}$$

where

$$M^{-1} = \frac{1}{|M|} \begin{pmatrix} K_{2T} & -K_{1T} \\ -K_{2\varepsilon} & K_{1\varepsilon} \end{pmatrix} \tag{8}$$

is the inverse matrix of coefficient matrix. $|M| = K_{1\epsilon}K_{2T} - K_{2\epsilon}K_{1T}$ is the determinant of the coefficient matrix. For the given wavelength measurement errors which are determined by the resolution

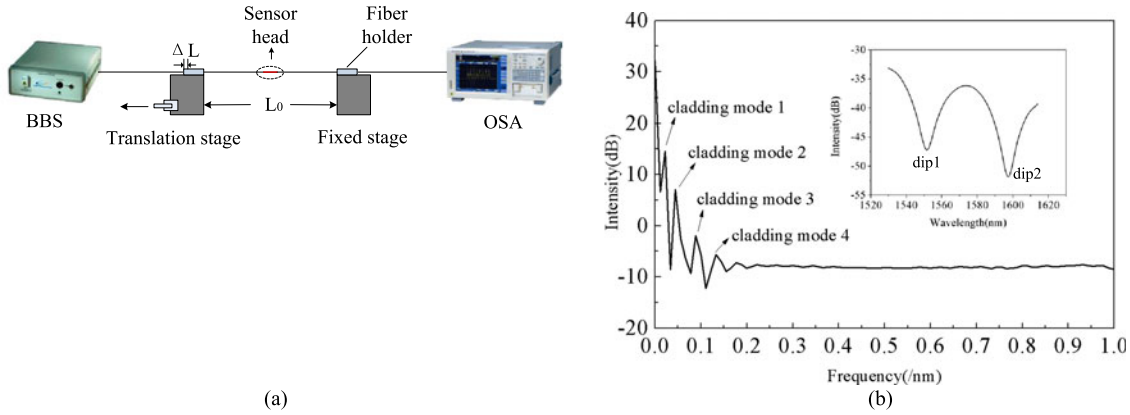

Fig. 4. (a) the experimental setup of strain measurement (b) the Fourier transform of the transmission spectrum. The inset is the transmission spectrum at room temperature.

of the optical spectrum analyzer (OSA), the tolerances of strain and temperature can be obtained by

$$\begin{pmatrix} \delta(\Delta\varepsilon) \\ \delta(\Delta T) \end{pmatrix} = abs(M^{-1}) \begin{pmatrix} \delta(\Delta\lambda_1) \\ \delta(\Delta\lambda_2) \end{pmatrix} \tag{9}$$

In this case, once the coefficient matrix is obtained through calibration, simultaneous measurement of strain and temperature can be easily achieved by monitoring the wavelength shifts of the resonant dips.

3. Experiment

Strain responses are tested by applying tensile stress on the Z-shape structure. A broadband light source (BBS) with the wavelength range from 1520 nm to 1610 nm is used as incident light and a optical spectrum analyzer (OSA: AQ6370c) with the highest resolution of 20 pm is used to record the transmission spectrum.

The experiments are conducted as depicted in Fig. 4(a). One fiber end is fixed on the block and another end is attached to a high-accuracy translation stage with a resolution of 10 μm. By adjusting the translation stage, we can vary the strain applied on the sensor. Appropriate pre-strain is applied to keep it straight. By doing this the influence of curvature can be avoided. And the transmission spectrum at room temperature is shown in the inset of Fig. 4(b). Two interference peaks–dip1 and dip2 can be observed clearly in the figure.

In order to understand the transmission characteristics of the sensor, Fast Fourier Transform (FFT) is conducted as shown in Fig. 4(b) to examine the interference patterns. Four dominant spatial frequency peaks are observed which indicate the interference between four cladding modes and core mode. Other weak interferences between the weak cladding modes and core mode slightly modulate the interference spectrum and can be ignored in the sensing applications.

The initial length between two fiber holders is denoted as L_0 and it is set to be 40 cm. The micro movement of translation stage is denoted as ΔL. We can calculate the axial strain inside the fiber by the formula

$$S = \frac{\Delta L}{L_0} \tag{10}$$

The strain is increased from 0 $\mu\epsilon$ to 300 $\mu\epsilon$ with a step of 25 $\mu\epsilon$.

As shown in Fig. 5(a), the resonant dips move to longer wavelength with strain increasing. The strain applied not only elongates the sensor but also changes the effective refractive index of core mode and cladding modes.

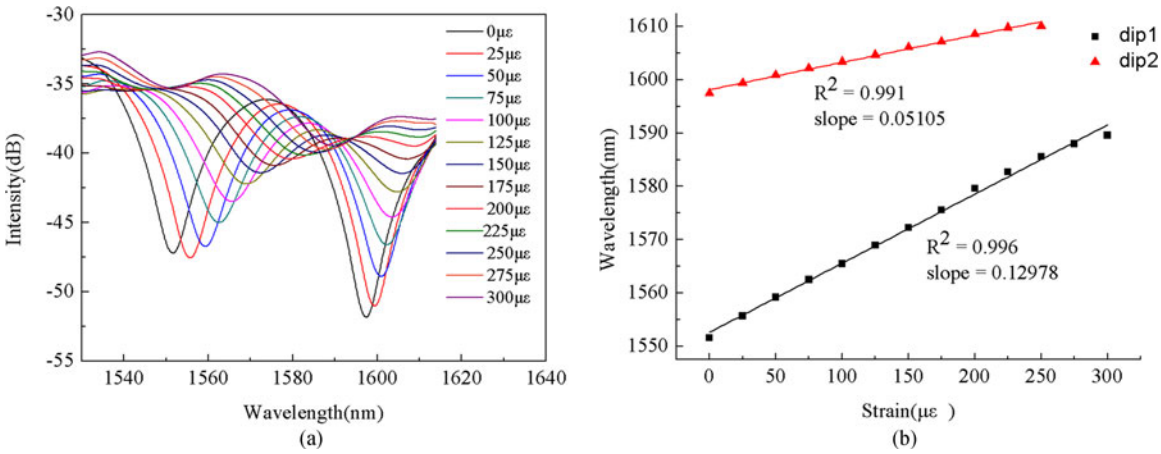

Fig. 5. (a) the shift of transmission spectrum with the augment of strain (b) the relationship between the wavelength shift and strain.

TABLE 1
Comparison of Sensing Performances of Different Structures

No.	Structure	Strain sensititvity (pm/$\mu\epsilon$)	Temperature sensititvity (pm/°C)	Ref.
1	Micro-tapered fiber grating	−0.55	49.6	[13]
2	Three core fiber cascaded with LPG	−2.96 / −1.52	42.9 / 47.4	[8]
3	Fiber taper and a lateral-shifted junction	−1.47/ −2.71	60.4 / 63.9	[6]
4	Cascading two sections of thin-core fiber	−1.03 / 0	30.74 / 20.48	[14]
5	Spheroidal-Cavity-overlapped FBG	1.4 / 3.76	8.4 / 0.67	[15]
6	Modal interferometer cascaded with FBG	−0.64 / 1.09	44.9 / 11.4	[16]
7	Multimode fiber cascaded with FBG	0.48 / 0.12	52 / 9	[17]
8	Z-shape fiber stucture	129.78 /51.05	43.57 / 62.10	This work

As the resonant wavelengths have red shift, the effective length L_{eff} must increase much faster than the decrease of the effective refractive index difference Δn_{eff}. Meanwhile, the sensor is elongated which causes less light energy leaking to the cladding. It means that the mode interference will be weakened.

As we can tell in Fig. 5(a), the depth of attenuation dips decreases with the augment of strain and it is coincided with theoretical analysis. Fig. 5(b) shows the relationship between the wavelength shifts and strain. The slopes of the curves give the sensitivities of 129.78 pm/$\mu\epsilon$ and 51.05 pm/$\mu\epsilon$, respectively. To the best of our knowledge, the strain sensitivity is relatively high compared with other kinds of sensors ever reported which are listed in Table 1.

The temperature influence on the resonant wavelength is measured. The sensor head is placed in a heating furnace with both ends fixed on the fiber holders to keep it straight. The transmission spectra are recorded for the temperatures from 25 °C to 55 °C in steps of 5 °C, as shown in Fig. 6(a). The resonant dips have red shift with temperature increasing. The relationship between the resonant wavelengths and temperature is given in Fig. 6(b). It turns out that the wavelength shifts exhibits good linearity and the temperature sensitivities of two dips are 43.57 pm/°C and 62.14 pm/°C, respectively.

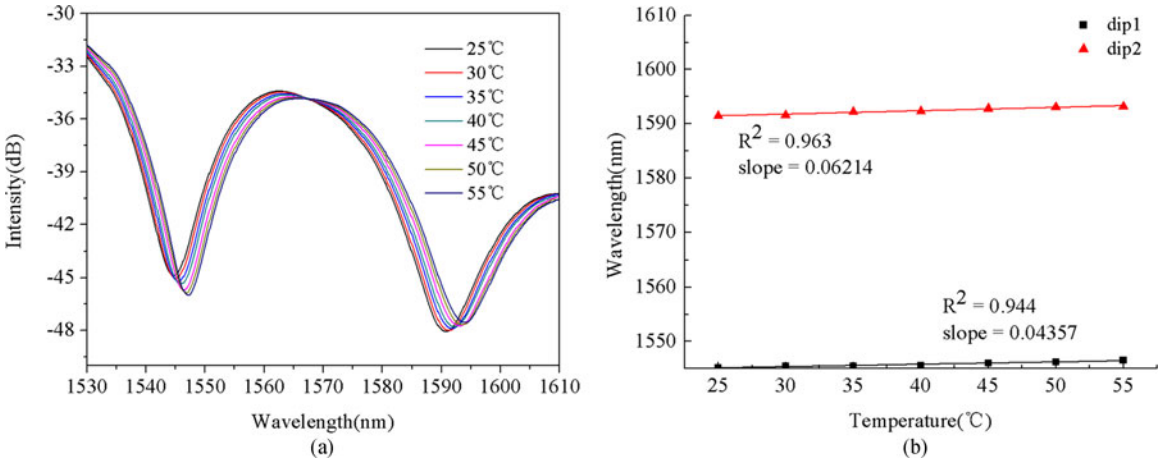

Fig. 6. (a) the shift of transmission spectrum with temperature increasing (b) the relationship between the wavelength shift and temperature.

According to the results, the matrix of the sensor can be expressed as

$$\begin{pmatrix} \Delta\lambda_1 \\ \Delta\lambda_2 \end{pmatrix} = \begin{pmatrix} 129.78 & 43.57 \\ 51.05 & 62.10 \end{pmatrix} \begin{pmatrix} \Delta\varepsilon \\ \Delta T \end{pmatrix} \tag{11}$$

$$\begin{pmatrix} \Delta\varepsilon \\ \Delta T \end{pmatrix} = \frac{1}{5835.09} \begin{pmatrix} 62.10 & -43.57 \\ -51.05 & 129.78 \end{pmatrix} \begin{pmatrix} \Delta\lambda_1 \\ \Delta\lambda_2 \end{pmatrix} \tag{12}$$

It can be seen from (12) that strain and temperature can be simultaneously measured by detecting the wavelength shifts of dip1 and dip2. For the given wavelength measurement error, the maximum strain and temperature tolerances can be calculated by (9). The performance of the sensor is tested by comparing the difference between the theoretical analysis and experimental results. The strain responses are measured in the range of 250 $\mu\varepsilon$ in a fixed temperature. Then the temperature responses are tested from 25 °C to 55 °C in a fixed strain. According to (12), the resolutions of strain and temperature are calculated to be $\pm$7.6 $\mu\varepsilon$ and $\pm$1.4 °C. It shows good agreement with theoretical analysis and the feasibility of the proposed structure can be confirmed.

4. Conclusion

In conclusion, an in-line all fiber Mach-Zehnder interferometer based on Z-shape structure is proposed here for the simultaneous measurement of strain and temperature. The structure is fabricated by exposing to CO_2 laser and it turns out that the special-designed structure is extremely sensitive to axial strain. The experiments show that the maximum strain sensitivity can reach up to 136.53 pm/$\mu\epsilon$ at room temperature. Furthermore, as the structure is fabricated without splicing or tapering, it is more robust compared to taper-based and spliced-based structures and it can be applicable for high strength sensing. Experiments demonstrate that the strain and temperature sensitivities of two dips are 129.78 pm/$\mu\epsilon$, 43.57 pm/°C and 51.05 pm/$\mu\epsilon$, 62.1 pm/°C. Thanks to the easy fabrication, stable performance and high sensitivity of the Z-shape structure, it has great potential to be applied in optical fiber sensing system.

References

[1] K. Ni *et al.*, "Miniature refractometer based on Mach–Zehnder interferometer with waist enlarged fusion bitaper," *Opt. Commun.*, vol. 292, pp. 84–86, Nov. 2012.

[2] Y. Cao *et al.*, "Simultaneous measurement of temperature and refractive index based on a Mach–Zehnder interferometer cascaded with a fiber Bragg grating," *Opt. Commun.*, vol. 342, pp. 180–183, Dec. 2014.

[3] L. M. Hu *et al.*, "Photonic crystal fiber strain sensor based on modified Mach–Zehnder interferometer," *IEEE Photon. J.*, vol. 4, no. 1, pp. 114–118, Feb. 2012.
[4] S. Zhang *et al.*, "Simultaneous measurement of relative humidity and temperature with PCF-MZI cascaded by fiber Bragg grating," *Opt. Commun.*, vol. 303, pp. 42–45, Apr. 2013.
[5] H. Gong *et al.*, "Simultaneous measurement of curvature and temperature based on Mach–Zehnder interferometer comprising core-offset and spherical-shape structures," *IEEE Photon. J.*, vol. 8, no. 1, Feb. 2016, Art. no. 6800109.
[6] P. Lu *et al.*, "Asymmetrical fiber Mach–Zehnder interferometer for simultaneous measurement of axial strain and temperature," *IEEE Photon. J.*, vol. 2, no. 6, pp. 942–953, Dec. 2010.
[7] D. Wu *et al.*, "All single-mode fiber Mach–Zehnder interferometer based on two peanut-shape structures," *IEEE J. Lightw. Technol.*, vol. 30, no. 5, pp. 805–810, Mar. 2012.
[8] T. Geng *et al.*, "Modal interferometer using three-core fiber for simultaneous measurement strain and temperature," *IEEE Photon. J.*, vol. 8, no. 4, Aug. 2016, Art. no. 6803908.
[9] K. Bhowmik *et al.*, "High intrinsic sensitivity etched polymer fiber Bragg grating pair for simultaneous strain and temperature measurements," *IEEE Sens. J.*, vol. 16, no. 8, pp. 2453–2459, Apr. 2016.
[10] H. Zeng *et al.*, "Combining two types of gratings for simultaneous strain and temperature measurement," *IEEE Photon. Technol. Lett.*, vol. 28, no. 4, pp. 477–480, Feb. 2016.
[11] B. H. Kim *et al.*, "Residual stress relaxation in the core of optical fiber by CO_2 laser irradiation," *Opt. Lett.*, vol. 26, no. 21, pp. 1657–1659, 2001.
[12] R. Yang *et al.*, "Single S-tapered fiber Mach–Zehnder interferometers," *Opt. Lett.*, vol. 36, no. 23, pp. 4482–4484, 2011.
[13] M.-S. Yoon *et al.*, "Simultaneous measurement of strain and temperature by using a micro-tapered fiber grating," *IEEE J. Lightw. Technol.*, vol. 30, no. 8, pp. 1156–1160, Apr. 2012.
[14] J. Shi *et al.*, "In-series singlemode thin-core diameter fibres for simultaneous temperature and strain measurement," *Electron. Lett.*, vol. 48, no. 2, pp. 93–95, Jan. 2012.
[15] Y. Pan *et al.*, "Simultaneous measurement of temperature and strain using spheroidal-cavity-overlapped FBG," *IEEE Photon. J.*, vol. 7, no. 6, Dec. 2015, Art. no. 6803406.
[16] Z. Cao *et al.*, "Compact fiber sensor with high spatial resolution for simultaneous strain and temperature measurement," *IEEE Sens. J.*, vol. 13, no. 5, pp. 1447–1551, May 2013.
[17] H. Sun, "Simultaneous measurement of temperature and strain or temperature and curvature based on an optical fiber Mach–Zehnder interferometer," *Opt. Commun.*, vol. 340, pp. 39–43, 2015.